

5 Supplemental Material

5.1 State-of-the-Art and TRL of Subsystems

5.1.1 Photovoltaic Devices and Modules

Electricity generation by solar cells using the photovoltaic effect has already achieved the highest technology level of TRL 9. Commercially-mature products have been on the market for more than a decade. Although numerous PV technologies exist, classified chiefly by the absorber material, the following discussion shall cover only the state-of-the art as far as commercially-available PV technologies are concerned. Crystalline silicon-based solar cells have the largest market share of PV modules. Within this technology path, p-type multi-crystalline silicon, using a combination of diffused junctions and a back surface field, predominate [1]. While the typical efficiency of commercial cells does not exceed 19%, a record efficiency of 22% was achieved for a 246 cm² multi-crystalline p-type silicon single wafer using passivated emitter rear cell (PERC) technology [2]. The highest present module efficiency of 20.4% has been reported for p-type mono-crystalline silicon, also based on PERC technology [3]. Even higher efficiencies have been achieved using n-type mono-crystalline silicon, which is believed to have a higher intrinsic efficiency limit than p-type silicon. At the time of writing this paper, the highest silicon efficiency values of 26.6% are reported for a 180 cm² single cell wafer [4] and 24.4% for a module with an area of 1.3 m² [5]. Here, the silicon heterojunction (SHJ) technology on n-type mono-crystalline silicon is used. Solar cells based on this technology are available on the market with efficiencies above 19.5% (see section 3.2.1). The recently reported efficiency record for small area solar cells based on p-type mono-crystalline silicon of 26.1% (4 cm²) [6] comes close to the highest efficiency values reported on a 180 cm² single cell wafer of 26.6% [4]. In summary, recent innovations in the PV device field have caused a growth in the market share of modules using mono-crystalline silicon because falling manufacturing cost have increased the effect of an efficiency gain on the levelized cost of electricity (LCOE) [1]. Moreover, higher efficiency values reduce the specific cost of the balance of system and, at the same time, increase the power output for the same module area. Thus, it is expected that PV-based STH efficiency is expected to increase and the cost will be reduced.

5.1.2 Electrolysis

The field of water electrolysis can be subdivided into three major technology pathways. Alkaline electrolysis is the most common technology with the highest market share and longest history of development [7, 8, 9]. There are installed systems with a nominal power exceeding 1 MW and system efficiencies of up to 80% (higher heating value) [10, 11]. A typical specific investment for this technology is reported to be 1100 \$/kW [12, 13]. Due to the high maturity of alkaline electrolysis systems, the TRL can be defined with a value of 9. Pressurized

electrolysis and operation at elevated temperature is considered to further improve the efficiency of alkaline electrolysis systems [14, 15]. Polymer electrolyte membrane (PEM), electrolysis, meanwhile, is the most anticipated technology for future applications. This is due to expected cost reductions, decreasing specific investment to 500 \$/kW and below as well as system efficiencies exceeding 80% (higher heating value) [16, 17, 18]. Specific investment costs at present are still in the range of 2000 \$/kW due to small market penetration [12, 13, 19]. There have been numerous setups demonstrating the technology at a nominal power level of several kW. Recently, this scale has been pushed by the launch of the Energiepark Mainz, which utilizes a PEM electrolyzer with a nominal output of 6 MW [17]. On the basis of this progress, the TRL of PEM technology can be estimated to be 8. Current research in the field of PEM electrolysis focuses on technological progress to achieve industrial readiness. This includes improved lifetime and durability of PEM stacks by investigating degradation mechanisms [20, 21]. Moreover, reduced catalyst-loading and gas-crossover through the membrane, increased system pressure as well as cost reductions through increased manufacturing volume are targets of current development efforts [12, 19, 22, 23, 24, 25]. Solid oxide electrolysis cells (SOE) operate at high-temperatures of between 600-900°C with higher system efficiencies than PEM electrolyzers, depending on how much waste heat from nearby processes can be integrated [26, 27, 28]. Currently, no commercial applications have been realized and laboratory-scale demonstrations are limited to nominal power levels of several kW. Therefore, the TRL of SOE electrolysis systems can be estimated to be 5. The approximated specific investment of solid oxide electrolysis ranges from 1000-4000 €, as the technology has not passed the state of laboratory research [29]. Recent research has focused on reducing degradation [30, 31, 32].

5.1.3 Concentrated Solar Power (CSP)

Solar Towers, parabolic troughs, solar dishes and linear Fresnel are the four concentrated solar power technologies (see Figure S1), which can deliver electricity – and heat if required – to the electrolyzer system.

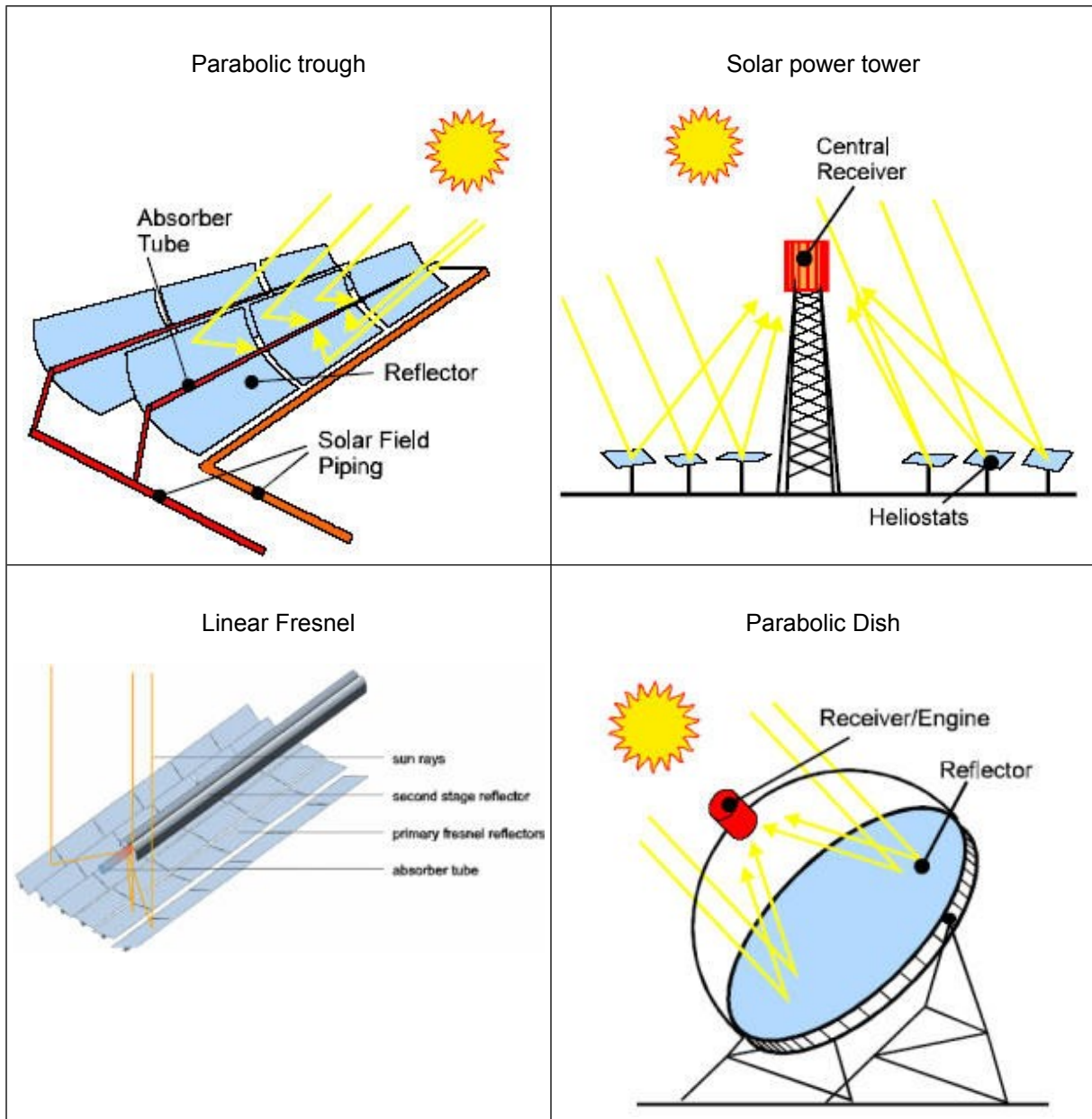


Figure S1. CSP technologies [33].

The solar tower technology is a large-scale system that utilizes many large, computer-controlled, sun-tracking mirrors, so-called heliostats, to focus sunlight on a receiver at the top of a tower. This receiver transforms the solar radiation into heat. A heat transfer fluid heated in the receiver then absorbs the highly concentrated radiation reflected by the heliostats and converts it into thermal energy. This heat is usually coupled to a conventional steam cycle through a heat exchanger to produce electricity. This technology enables operation at a high temperature level and provides heat storage capacities. Solar towers typically stand about 75-150 m height [34]. These plants are best suited for utility-scale applications in the 10-200 MW_e range [35]. This technology is commercially proven. The process design of the plant depends on the heat transfer fluid, which can be water, molten salt or air. In this study, the focus is on molten salt solar towers due to its superior energy storage capacity. In a molten salt solar tower, the heat transfer fluid used in the solar receiver to convert the collected solar

radiation into heat consists of molten salt which is typically a mixture, by-weight, of 60% sodium nitrate and 40% potassium nitrate. The molten salt is pumped from a large storage tank to the receiver at the top of the tower, where it is heated in tubes to a temperature of 565 °C. The hot salt is then returned to a second large storage tank where it remains until needed by the utility. At this point, the salt is pumped through a steam generator to produce the steam to power a conventional, high-efficiency steam turbine to produce electricity. Then, the cooled salt returns at a temperature of 285 °C to the first storage tank to be used in the cycle again. Due to the long-term molten salt thermal storage system that is normally integrated in these kinds of plants, it is possible to achieve 24 h operation during summer. Molten salts are indeed suitable for long-term storage due to their high thermal density and fluid properties at high temperature. The directly included storage system typically comprises a two-tank system: a “cold” one and a “hot” one. The molten salts from the “cold” tank feeds the solar receiver, are heated up and sent to the “hot” tank. As the steam generator is independently fed from the hot tank, the thermal storage system works as a buffer during solar transients and periods of no irradiance, so that the steam turbine’s operating conditions are stable. Thus, the first commercial molten salt power tower by Torresol Gemasolar can supply 15-hour full load equivalent heat storage capacity for a plant capacity of 12 MW_e [36]. As this plant is commercially-operated, it can be estimated that electricity generation by a molten salt solar power tower has achieved a high TRL of 9.

5.1.4 Photoelectrochemical (PEC) Water-Splitting

In photoelectrochemical solar-driven water-splitting, light harvesting and hydrogen generation are combined into a single monolithic device. In such devices, incident sunlight is converted into hydrogen using purely internally-biased electrolysis. Since at least one of the semiconductor surfaces is in contact with the electrolyte, the capital cost of a separate electrolyzer is avoided, potentially reducing the cost of the balance of plant, provided that chemically-stable materials are available.

One way to increase STH efficiency has been to use multi-junction semiconductors consisting of a photocathode and a photoanode to increase the utilization of incident photons, with an STH value of 8.2% reported [37]. Nevertheless, devices utilizing photoelectrodes are still at a low technology readiness level, as materials must still be found that best optimize the requirement for maximum utilization of the spectrum, a high open circuit voltage and long-term resistance to photoelectrochemical corrosion. Moreover, very few reports of solar-driven water-splitting devices based purely on photoelectrodes, of sizes approaching the m² range that would attract commercial interest, are available [38].

Yet, higher solar-to-hydrogen efficiencies approaching 10% have been achieved by using PV-PEC hybrid devices where the photovoltaic junction provides an additional bias, albeit at a higher material cost [39, 40]. Other options completely omit the use of photoelectrodes and instead monolithically-integrated, multijunction PV devices with electrocatalysts are used [41], achieving higher STH efficiency values of 10-22%. The highest STH efficiencies of devices measuring at least 50 cm² and using monolithically-integrated PV with electro-catalysts are,

however, still below 10% [42]. Despite the strides made in STH efficiency over the years, the device stability remains challenging and is the biggest barrier to large-scale deployment of PEC and related technologies for water-splitting. Therefore, we categorize these approaches as having a technology readiness level of 3 because the proof of concept has been shown but stability in both the laboratory and operational environment has not yet been validated.

5.2 Irradiance profiles of all locations considered in this study

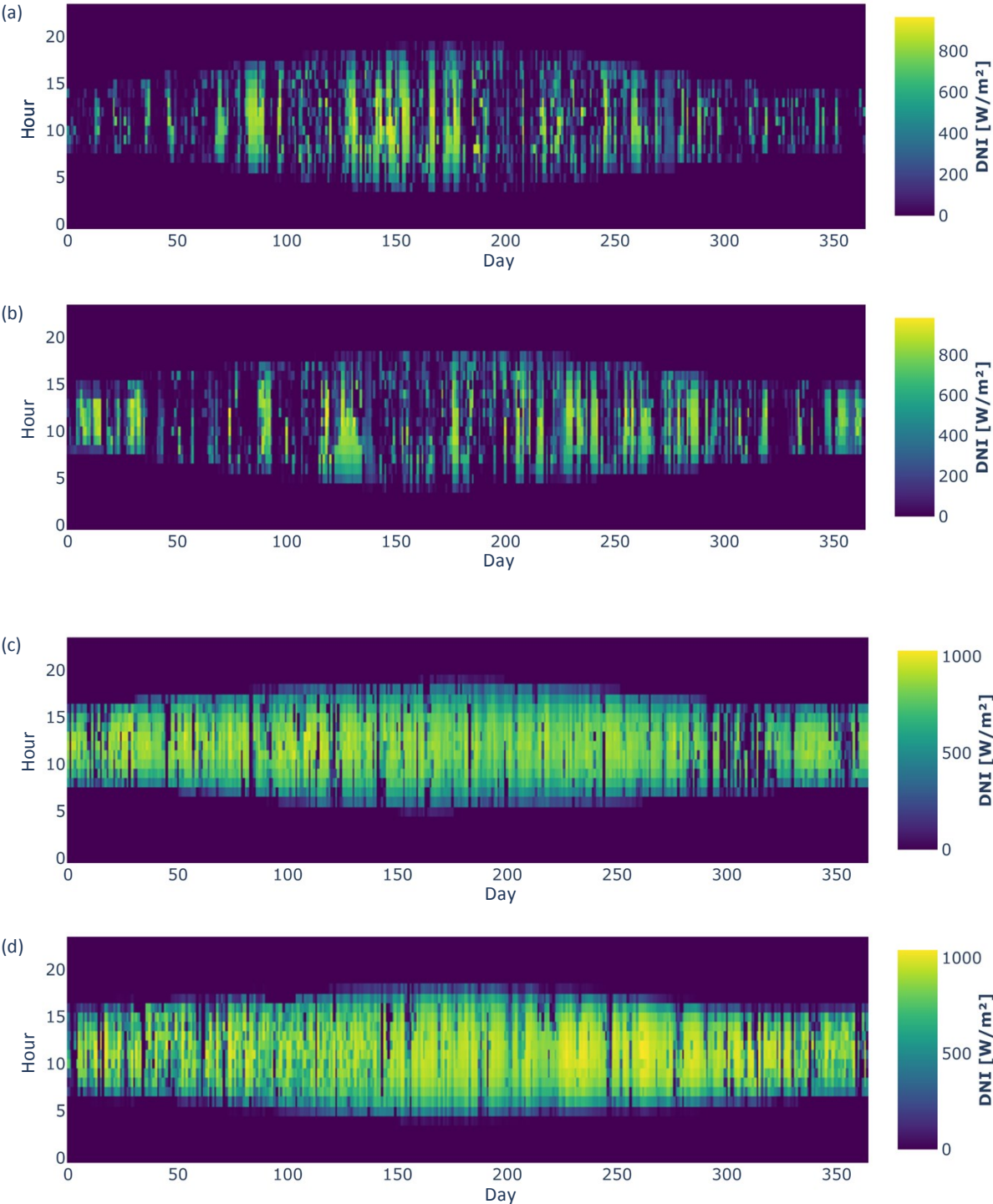


Figure S2. Irradiance profiles for Oldenburg/Germany (a), Freiburg/Germany (b), (c) Almeria/Spain (c) and Daggett/USA (d).

5.3 Hydrogen production quantities per location

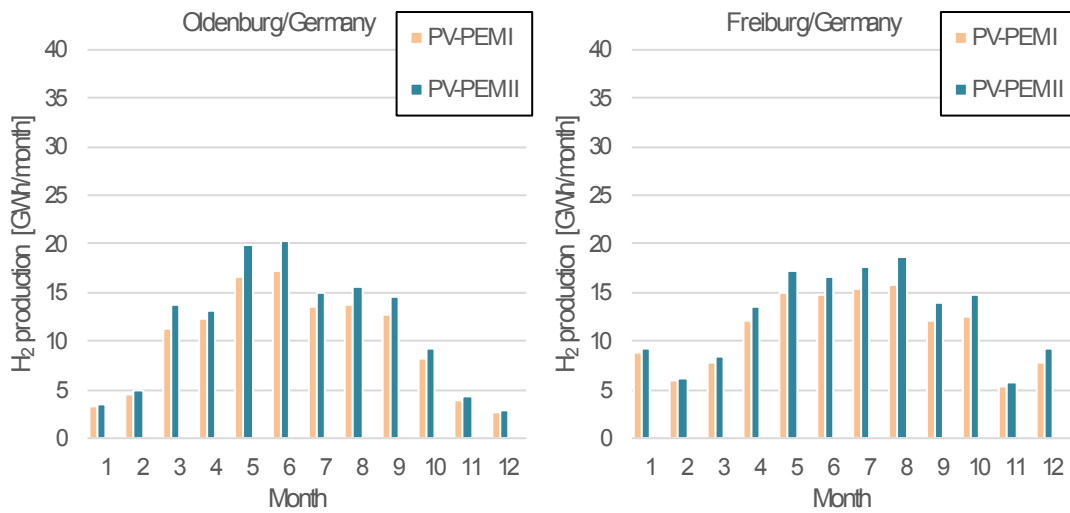


Figure S3. Annual hydrogen production quantities in Oldenburg and Freiburg in Germany (PV-PEM concepts only).

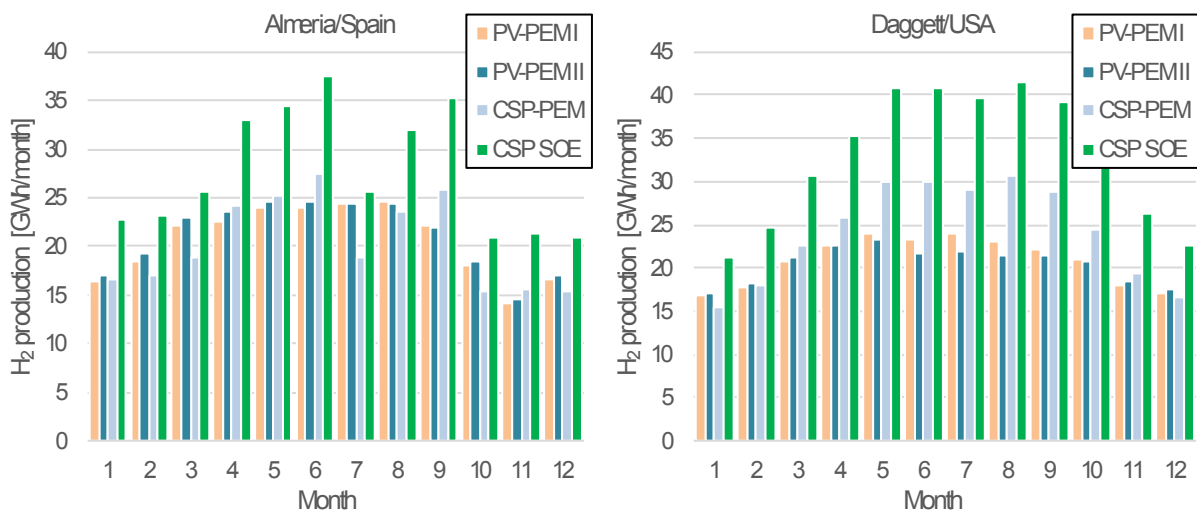


Figure S4. Annual hydrogen production quantities in Almeria/Spain and Daggett/USA (all concepts).

5.4 Sensitivity Analysis

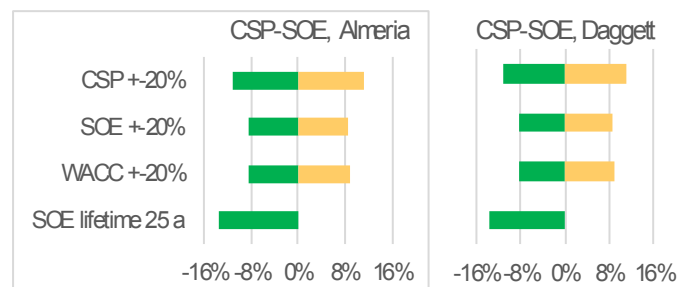


Figure S5. Cost sensitivities of the CSP-SOE for Almeria/Spain and Daggett/USA with unchanged conversion efficiency.

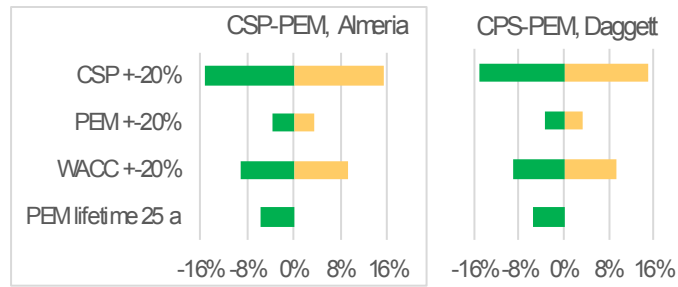


Figure S6. Cost sensitivities of the CSP-PEM for Almeria/Spain and Daggett/USA.

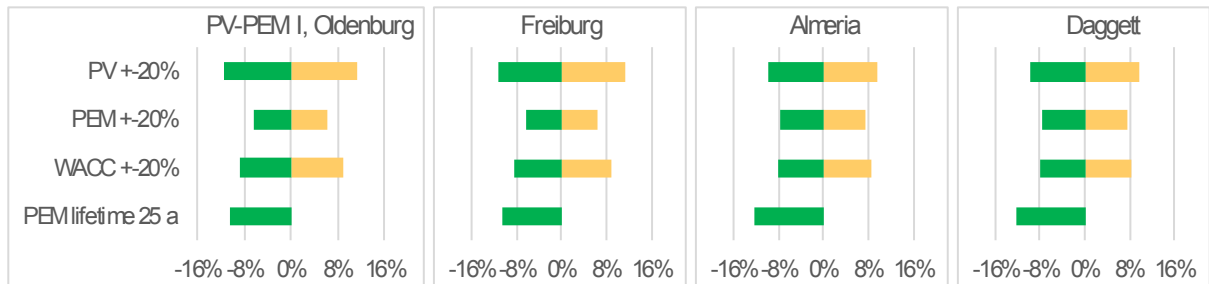


Figure S7. Cost sensitivities of the PV-PEM I for all locations.

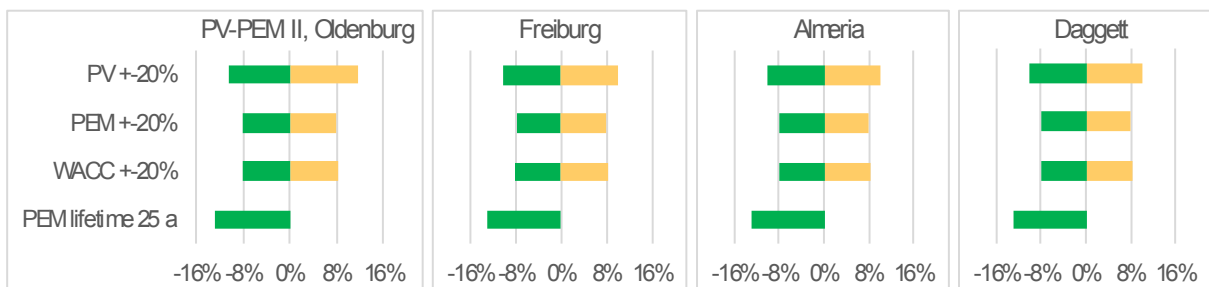


Figure S8. Cost sensitivities of the PV-PEM II for all locations.

5.5 Cost reduction potential

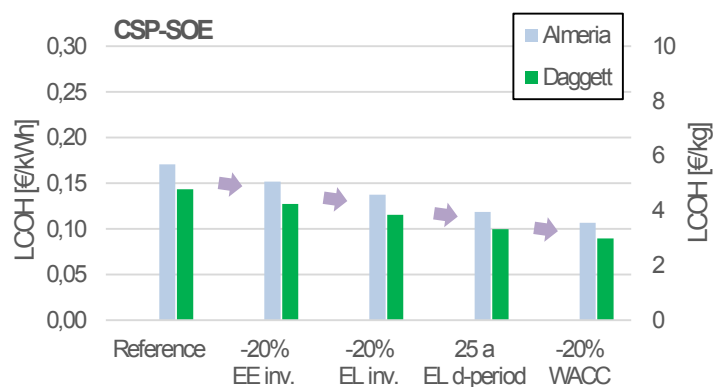


Figure S9. Cost reduction potential of the CSP-SOE concept with the energy conversion efficiency kept constant.

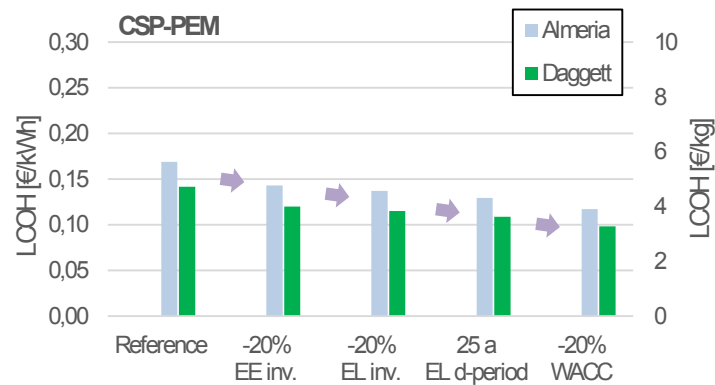


Figure S10. Cost reduction potential of the CSP-PEM concept with the energy conversion efficiency kept constant.

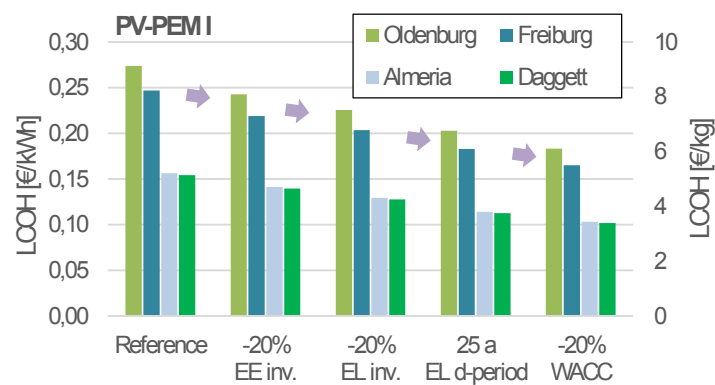


Figure S11. Cost reduction potential of the PV-PEM I concept with the energy conversion efficiency kept constant.

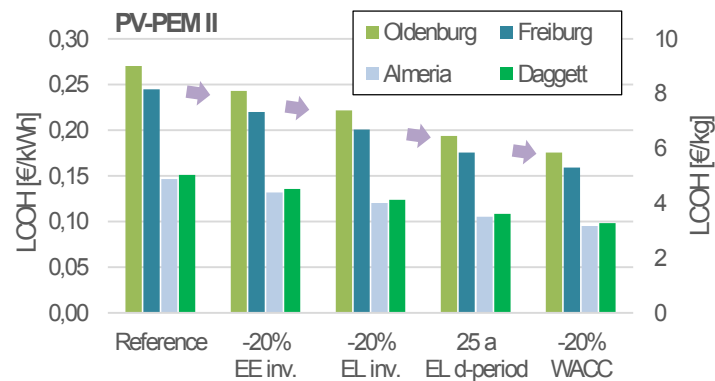


Figure S12. Cost reduction potential of the PV-PEM II concept with the energy conversion efficiency kept constant.

References

1. International Technology Roadmap for Photovoltaic, 2015.
2. Publicover, B., JinkoSolar claims new 22.78% PERC efficiency record, in PV Magazine2017.
3. Solar, L., Conversion Efficiency at 20.41%, LONGi Solar Creates World Record of Monocrystalline PERC Module, 2018.

4. New World Record Established for Conversion Efficiency in a Crystalline Silicon Solar Cell, 2017, Kaneka Corporation.
5. Corporation, K., World's Highest Conversion Efficiency of 24.37% Achieved in a Crystalline Silicon Solar Cell Module, 2017.
6. 26.1% record efficiency for p-type crystalline Si solar cells. 2018 [cited 2018 06 Feb]; Available from: <https://isfh.de/en/26-1-record-efficiency-for-p-type-crystalline-si-solar-cells/>.
7. Zeng, K. and D. Zhang, Recent progress in alkaline water electrolysis for hydrogen production and applications. *Progress in Energy and Combustion Science*, 2010. **36**(3): p. 307-326, DOI: 10.1016/j.pecs.2009.11.002.
8. Holladay, J.D., J. Hu, D.L. King, and Y. Wang, An overview of hydrogen production technologies. *Catalysis Today*, 2009. **139**(4): p. 244-260, DOI: 10.1016/j.cattod.2008.08.039.
9. Manabe, A., M. Kashiwase, T. Hashimoto, T. Hayashida, A. Kato, K. Hirao, I. Shimomura, and I. Nagashima, Basic study of alkaline water electrolysis. *Electrochimica Acta*, 2013. **100**: p. 249-256, DOI: 10.1016/j.electacta.2012.12.105.
10. Barisic, M., *Alkalische Elektrolyse in der Industriellen Anwendung*, 2012, ELB Elektrolysetechnik.
11. Chakik, F.e., M. Kaddami, and M. Mikou, Effect of operating parameters on hydrogen production by electrolysis of water. *International Journal of Hydrogen Energy*, 2017. **42**(40): p. 25550-25557, DOI: 10.1016/j.ijhydene.2017.07.015.
12. Babic, U., M. Suermann, F.N. Büchi, L. Gubler, and T.J. Schmidt, Critical Review—Identifying Critical Gaps for Polymer Electrolyte Water Electrolysis Development. *Journal of The Electrochemical Society*, 2017. **164**(4): p. F387-F399, DOI: 10.1149/2.1441704jes.
13. Smolinka, T., M. Günther, and J. Garche, NOW-Studie: Stand und Entwicklungspotenzial der Wasserelektrolyse zur Herstellung von Wasserstoff aus regenerativen Energien, 2011, Fraunhofer ISE.
14. Ganley, J.C., High temperature and pressure alkaline electrolysis. *International Journal of Hydrogen Energy*, 2009. **34**(9): p. 3604-3611, DOI: 10.1016/j.ijhydene.2009.02.083.
15. Allebrod, F., C. Chatzichristodoulou, and M.B. Mogensen, Alkaline electrolysis cell at high temperature and pressure of 250 °C and 42 bar. *Journal of Power Sources*, 2013. **229**: p. 22-31, DOI: 10.1016/j.jpowsour.2012.11.105.
16. Bhandari, R., C.A. Trudewind, and P. Zapp, Life cycle assessment of hydrogen production via electrolysis – a review. *Journal of Cleaner Production*, 2014. **85**: p. 151-163, DOI: 10.1016/j.jclepro.2013.07.048.
17. Kopp, M., D. Coleman, C. Stiller, K. Scheffer, J. Aichinger, and B. Scheppat, *Energiepark Mainz: Technical and economic analysis of the worldwide largest Power-*

- to-Gas plant with PEM electrolysis. *International Journal of Hydrogen Energy*, 2017, DOI: 10.1016/j.ijhydene.2016.12.145.
18. Olivier, P., C. Bourasseau, and P.B. Bouamama, Low-temperature electrolysis system modelling: A review. *Renewable and Sustainable Energy Reviews*, 2017. **78**: p. 280-300, DOI: 10.1016/j.rser.2017.03.099.
 19. Carmo, M., D.L. Fritz, J. Mergel, and D. Stolten, A comprehensive review on PEM water electrolysis. *International Journal of Hydrogen Energy*, 2013. **38**(12): p. 4901-4934, DOI: <http://dx.doi.org/10.1016/j.ijhydene.2013.01.151>.
 20. Chandesris, M., R. Vincent, L. Guetaz, J.S. Roch, D. Thoby, and M. Quinaud, Membrane degradation in PEM fuel cells: From experimental results to semi-empirical degradation laws. *International Journal of Hydrogen Energy*, 2017. **42**(12): p. 8139-8149, DOI: 10.1016/j.ijhydene.2017.02.116.
 21. Ozden, E. and I. Tari, PEM fuel cell degradation effects on the performance of a stand-alone solar energy system. *International Journal of Hydrogen Energy*, 2017. **42**(18): p. 13217-13225, DOI: 10.1016/j.ijhydene.2017.04.017.
 22. Ayers, K.E., J.N. Renner, N. Danilovic, J.X. Wang, Y. Zhang, R. Maric, and H. Yu, Pathways to ultra-low platinum group metal catalyst loading in proton exchange membrane electrolyzers. *Catalysis Today*, 2016. **262**: p. 121-132, DOI: 10.1016/j.cattod.2015.10.019.
 23. Whitney G. Colella, B.D.J., Jennie M. Moton, Genevieve Saur, Todd Ramsden, *Techno-economic Analysis of PEM Electrolysis for Hydrogen Production*. 2014,
 24. Bensmann, B., R. Hanke-Rauschenbach, and K. Sundmacher, In-situ measurement of hydrogen crossover in polymer electrolyte membrane water electrolysis. *International Journal of Hydrogen Energy*, 2014. **39**(1): p. 49-53, DOI: 10.1016/j.ijhydene.2013.10.085.
 25. Schalenbach, M., M. Carmo, D.L. Fritz, J. Mergel, and D. Stolten, Pressurized PEM water electrolysis: Efficiency and gas crossover. *International Journal of Hydrogen Energy*, 2013. **38**(35): p. 14921-14933, DOI: 10.1016/j.ijhydene.2013.09.013.
 26. Peters, R., R. Deja, L. Blum, V.N. Nguyen, Q. Fang, and D. Stolten, Influence of operating parameters on overall system efficiencies using solid oxide electrolysis technology. *International Journal of Hydrogen Energy*, 2015. **40**(22): p. 7103-7113, DOI: 10.1016/j.ijhydene.2015.04.011.
 27. Fang, Q., L. Blum, and N.H. Menzler, Performance and Degradation of Solid Oxide Electrolysis Cells in Stack. *Journal of the Electrochemical Society*, 2015. **162**(8): p. F907-F912, DOI: 10.1149/2.0941508jes.
 28. Klotz, D., A. Leonide, A. Weber, and E. Ivers-Tiffée, Electrochemical model for SOFC and SOEC mode predicting performance and efficiency. *International Journal of Hydrogen Energy*, 2014. **39**(35): p. 20844-20849, DOI: 10.1016/j.ijhydene.2014.08.139.

29. Schmidt, O., A. Gambhir, I. Staffell, A. Hawkes, J. Nelson, and S. Few, Future cost and performance of water electrolysis: An expert elicitation study. *International Journal of Hydrogen Energy*, 2017. **42**(52): p. 30470-30492, DOI: 10.1016/j.ijhydene.2017.10.045.
30. Tietz, F., D. Sebold, A. Brisse, and J. Schefold, Degradation phenomena in a solid oxide electrolysis cell after 9000 h of operation. *Journal of Power Sources*, 2013. **223**(Supplement C): p. 129-135, DOI: <https://doi.org/10.1016/j.jpowsour.2012.09.061>.
31. Chatzichristodoulou, C., M. Chen, P.V. Hendriksen, T. Jacobsen, and M.B. Mogensen, Understanding degradation of solid oxide electrolysis cells through modeling of electrochemical potential profiles. *Electrochimica Acta*, 2016. **189**(Supplement C): p. 265-282, DOI: <https://doi.org/10.1016/j.electacta.2015.12.067>.
32. Schiller, G., M. Hörlein, and A. Nechache, Detailed Study of Degradation Behavior of Solid Oxide Cells in Electrolysis and Co-Electrolysis Mode, 2016, German Aerospace Center (DLR).
33. <http://www.solarpaces.org/how-csp-works/>. 09.03.2018].
34. Barlev, D., R. Vidu, and P. Stroeve, Innovation in concentrated solar power. *Solar Energy Materials and Solar Cells*, 2011. **95**(10): p. 2703-2725,
35. Romero, M. and A. Steinfeld, Concentrating solar thermal power and thermochemical fuels. *Energy & Environmental Science*, 2012. **5**(11): p. 9234, DOI: 10.1039/c2ee21275g.
36. Dunn, R.I., P.J. Hearps, and M.N. Wright., Molten-salt power towers: newly commercial concentrating solar storage, in *IEEE2012*.
37. R. C. Kainthla, B.Z., J. O'M. Bockris, Significant efficiency increase in self-driven photoelectrochemical cell for water photoelectrolysis. *Journal of the Electrochemical Society*, 1987. **134** (4): p. 841-845,
38. Artiphyction. Fully artificial photo-electrochemical device for low temperature hydrogen production. 2018 [cited 2018 12 Feb]; Available from: <http://www.artiphyction.org>.
39. Kim, J.H., Y. Jo, J.H. Kim, J.W. Jang, H.J. Kang, Y.H. Lee, D.S. Kim, Y. Jun, and J.S. Lee, Wireless Solar Water Splitting Device with Robust Cobalt-Catalyzed, Dual-Doped BiVO₄ Photoanode and Perovskite Solar Cell in Tandem: A Dual Absorber Artificial Leaf. *ACS Nano*, 2015. **9**(12): p. 11820-11829, DOI: 10.1021/acs.nano.5b03859.
40. Kim, J.H., J.-W. Jang, Y.H. Jo, F.F. Abdi, Y.H. Lee, R. van de Krol, and J.S. Lee, Hetero-type dual photoanodes for unbiased solar water splitting with extended light harvesting. *Nature Communications*, 2016. **7**(1): p. 13380, DOI: 10.1038/ncomms13380.
41. Walczak, K.A., G. Segev, D.M. Larson, J.W. Beeman, F.A. Houle, and I.D. Sharp, Hybrid Composite Coatings for Durable and Efficient Solar Hydrogen Generation under Diverse Operating Conditions. *Advanced Energy Materials*, 2017. **7**(13): p. 1602791, DOI: 10.1002/aenm.201602791.

42. Becker, J.P., B. Turan, V. Smirnov, K. Welter, F. Urbain, J. Wolff, S. Haas, and F. Finger, A modular device for large area integrated photoelectrochemical water-splitting as a versatile tool to evaluate photoabsorbers and catalysts. *J. Mater. Chem. A*, 2017, DOI: 10.1039/c6ta10688a.